Received: 4 August 2020 | Revised: 15 September 2020 | Accepted: 11 October 2020

DOI: 10.1002/jbio.202000318

FULL ARTICLE

JOURNAL OF BIOPHOTONICS

SERS-based sensor for direct L-selectin level determination in plasma samples as alternative method of tumor detection

Aneta Aniela Kowalska* | **Ariadna B. Nowicka** | **Tomasz Szymborski** | **Patrycja Piecyk** | **Agnieszka Kamińska***

Institute of Physical Chemistry, Polish Academy of Sciences, Warsaw, Poland

***Correspondence**
Aneta Aniela Kowalska and Agnieszka Kamińska, Institute of Physical Chemistry, Polish Academy of Sciences, Kasprzaka 44/52, 01-224 Warsaw, Poland.
Email: akowalska@ichf.edu.pl (A. A. K.)
and
Email: akaminska@ichf.edu.pl (A. K.)

Funding information
Narodowe Centrum Nauki, Grant/Award Number: OPUS XIII 2017/25/B/ST4/01109

Abstract

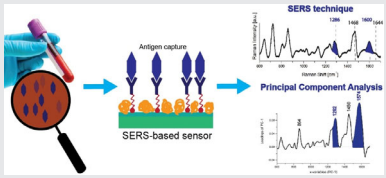

Selectin ligands are present on the surface of tumor cells, for this reason lowering the L-selectin level in the blood and lymph can indicate presence of the tumor. Therefore the selectin level in the plasma are potential targets for anticancer therapy. We demonstrate the surface enhanced Raman spectroscopy (SERS)-based sensor for the determination of L-selectin level in biological samples that can be used in medical diagnosis. The combination of SERS with the method of multivariate analysis as principle component analysis (PCA) allows to strengthen the presented data analysis. The loadings of PCA permit to indicate those vibration modes, that are the most important for the assumed identification (bands at 1574, 1450, 1292 cm^{-1}). Two bands at 1286 and 1580 cm^{-1} were selected for the determination of the calibration curve (bands intensities I_{1286}/I_{1580} ratio). The L-selectin level of biological samples can be read, directly from the calibration curve. The presented sensor is as a sensitive tool with good specificity and selectivity of L-selectin, even in the case of coexistence of P- and E-selectin.

KEYWORDS

L-selectin, SERS platform, surface enhanced Raman spectroscopy, tumor

1 | INTRODUCTION

Growing knowledge of the immune system and recent advances in technology allows for better understanding of the host defending system. The immune system can lead to antitumor response and elimination of tumor cells, as recognizes and attacks the potentially harmful substances by responding to their antigens. Leukocyte recruitment to sites of inflammation or infection is mediated by highly specific receptor–ligand interactions provided by adhesion molecules, such as chemokines, integrins and selectins.[1] Selectins are members of the C-type lectin family of cell adhesion molecules. Among them, E-selectin expression is induced on endothelium and requires de novo mRNA and protein synthesis. P-selectin is rapidly translocated to the cell surface from intracellular storage granules in activated endothelium and in platelets. L-selectin is constitutively expressed on the surface of almost all types of leukocytes (T and B, natural killer, macrophage/monocyte, granulocyte cells) and allows leukocytes to leave the bloodstream, make random contacts and tether to activated endothelial cells, where rolling and finally adhere to cells.[2–4] The absence of selectins can lead to reduced neutrophil recruitment to sites of inflammation, impaired lymphocyte trafficking, and decreased leukocyte turnover.[5–7] Moreover, the selectin family of adhesion molecules plays a prominent role in

immune/inflammatory responses[8, 9] but also in stroke[10] and progression of cancer.[8, 11] Selectins were shown to mediate T cell recruitment both to the lymph node and/or to the tumor sites, but also myeloid-derived cells to tumors. The higher level of selectin ligands on tumor cells is linked to cancer-associated aberrant glycosylation that makes selectins potential targets for cancer therapy.[12, 13] Furthermore, other lectin binding molecules, such as Siglec (a subset of the I-type lectins) may modify immune responses during cancer.[14] The increased selectin ligand expression on tumor cells correlates with enhanced metastasis and poor prognosis for individuals.

During inflammation, L-selectin mediates leukocyte-leukocyte interaction using leukocyte P-selectin glycoprotein ligand-1.[15] Deficiency of L-selectin significantly reduce in inflammation due to the loss of these interactions and L-selectin on incoming leukocytes.[16] In tumor, the selectin-dependent mechanisms mediating cell tethering and rolling interactions through recognition of carbohydrate ligands on tumor cell to enhance distant organ metastasis.[17] Selectins contribute to leukocyte recruitment at metastatic and premetastatic sites of tumor diseases and the concentration of selectin which are very important for healing process. It is known, that partial inhibition of selectin function might increase host immune-defense.[8] Moreover, the selectin molecules, are involved in the pathogenesis of various central nervous system illnesses, such as bacterial meningitis,[18] encephalitis,[19] and cerebral ischaemia.[20] The amount of L-selectin in the tumor samples may vary in the wide range, as can decrease or increase according to the state or disease progression. In the ovarian cancer[21] or the urothelial carcinoma[22] the level of L-selectin decrease with disease progression. In a healthy person, a concentration of L-selectin in plasma can be found in the range of 700 to 1500 ng mL^{-1}.[23] Nowadays, commercially available ELISA kits for human L-selectin determination in serum, plasma and cell culture supernatants can be used for determination of selectin in narrow region (e.g. 0.625–4, 1–20 or 1–58 ng mL^{-1}). ELISA analyses are based on rather long preparation (up to 12 hours) and colorimetric technique, also before beginning the ELISA protocol, biological samples require the determination of the dilution ratio (usually from 100 to 1000), which further extend the time and make it difficult to directly determine the L-selectin level in serum or plasma samples. Therefore, it is important to develop sensing systems to detect L-selectin at low (below 700 ng mL^{-1}) as well test, which allows for direct determination of L-selectin level in biological samples (without dilution pretreatment step determination), what finally permits to make early-stage tumor diagnosis, and further in patients with tumor, to make possible their positive medical treatment.[24] In conclusion, the question of how L-selectin contributes to the control or weakening of the particular tumors or viruses remains open. Determining the level of L-selectin in various biological samples may help to understand the L-selectin clustering what can enhance T-cell receptor signaling, suggesting roles further than just trafficking.[25]

Surface enhanced Raman spectroscopy (SERS) offers fast detection and identification of different chemical and biological analytes. The enhancement of Raman signals of adsorbed molecules is realized on specially prepared metal nanostructures or nanoparticles and attributed to the electromagnetic and chemical mechanisms. Calculated enhancement factor (EF) for Raman signal can reach 10^{12}.[26] Therefore SERS offers fast detection and identification of different chemical and biological analytes up to single molecule.[27] Till now SERS has been employed for analyzing complex biological molecules from whole proteins,[27] peptides,[28] DNA,[29] bacteria[30] and viruses[31] but also such moieties as circulating tumor cells[32] or neoplastic diseases.[33]

In the framework of this work the ultrasensitive and reliable L-selectin sensor based on SERS technique is presented. The biggest challenge in the fabrication of SERS-based sensors is to prepare a substrate specially dedicated to the studied analytes as well as to elaborate an appropriate method of antigen capture, that allows for qualitative and quantitative analysis of studied analyte. Fabricated sensor is based on silicon covered with Au/Ag layer especially modified for the L-selectin level determination. In this work, we present SERS sensor for direct L-selectin detection from clinical samples along with its sensitivity, selectivity and specificity characterization.

2 | EXPERIMENTAL

2.1 | Chemicals and materials

L-selectin, P-selectin, E-selectin human protein (CD62L, CD62P, CD62E) and the L-selectin antibody were obtained from Tocris Bioscience (Bristol, UK). The thiolated polyethylene glycol (PEG-NHS) ester disulfide was purchased from Polypure (Norway). Phosphate-buffered saline (PBS) packs (10 mM, pH = 7.2) from Sigma–Aldrich (Dorset, UK) were used without further purification. Water purified using a Milli-Q plus 185 system with resistivity over 18 MΩ was used throughout experiments.

For the method of L-selectin level evaluation we used the plasma samples gathered from two patients with the adenocarcinoma of the lung (accordingly to World Health Organization, stage IV) and one plasma from the

healthy patient. Clinical samples (three in total) were available by courtesy of Medical University of Lublin, Department of Pneumonology, Oncology and Allergology (Lublin, Poland). Additionally, those plasma samples were studied for L-selectin level using the commercial enzyme-linked immunosorbent assay (ELISA, Sigma–Aldrich), according to Sigma–Aldrich procedure.

All experiments performed for clinical samples were performed in compliance with the relevant laws and institutional guidelines. The protocol of study was approved by the Ethics and Bioethics Committee of Cardinal Stefan Wyszyński University in Warsaw (Poland).

2.2 | SERS platform fabrication and characterization

The SERS surfaces were prepared based on a simple protocol according to patent application.[34] Briefly, first the silicon wafers were prepared by the laser ablation with the fundamental (1030 nm) wavelength of a compact fiber chirped-pulse amplification system set in a single pass configuration, where the active medium of the oscillator was Yb:KYW crystal (repetition rate 300 kHz, pulse width 300 fs). Then, the surfaces were sputtered with gold/silver (Au/Ag alloy) layer using the PVD equipment (Quorum, Q150T ES, Laughton, UK). The Au/Ag target in the ratio 30/70 were supplied from Mennica Metale Szlachetne (Warsaw, Poland). The target diameter and thickness was 58 mm and 0.25 mm, respectively. The sputtering current was 25 mA and the vacuum during the silver sputtering was on the level of 10^{-2} mbar (the argon pressure applied for this equipment is equal to 0.4 bar). The thickness of the sputtered layer was controlled with an embedded quartz microbalance.

Silicon after layer ablation were covered layer of gold/silver with a thickness of 70 nm. The SERS platforms were then placed in a sterile Petri dish. The obtained Au/Ag SERS surfaces were characterized using SEM images taken with a FEI Nova NanoSEM 450 scanning electron microscope (Hillsboro, OR, USA), where the accelerating voltage was 5 or 10 kV. The samples of Au/Ag SERS substrates were attached to SEM stabs with carbon tape.

2.3 | Protocol of the antibody immobilization

SERS substrates after ablation and covered with Au/Ag layer were further used for SERS-based sensor fabrication (Figure 1). First, SERS substrates were cleaned by ozone plasma washing generated by the corona treater (Figure 1A). Then, such a freshly ozone-cleaned SERS substrates were modificated with PEG-NHS, providing a chemical group suitable for covalent binding with a primary amine group in an antibody (or another protein) (Figure 1B). Treatment of substrates with solution containing both the amino and thiol groups is necessary to

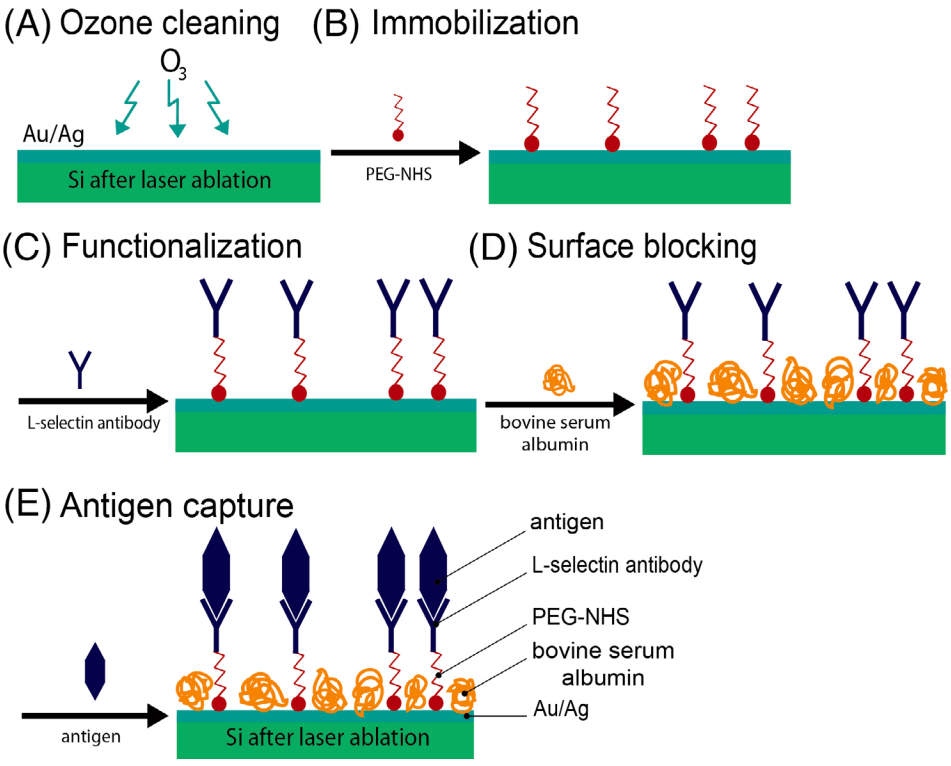

FIGURE 1 The schematic view of the applied protocol for L-selectin antigen capture. The protocol consist of five steps. After ozone cleaning SERS platforms, A; the PEG-NHS immobilization is performed, B; then L-selectin antibody is functionalized onto the platform, C. The reaming free places on the platform are blocked by bovine serum albumin, D. The last step is the antigen captured from the samples containing L-selectin using prepared SERS-sensor, E. PEG-NHS, thiolated polyethylene glycol; SERS, surface enhanced Raman spectroscopy

incorporate functional groups or molecules that facilitate linkage of the surface for the antibody immobilization. In the next step (functionalization) the monoclonal L-selectin antibody was attached and stopped onto PEG-NHS immobilized SERS substrates by bond covalent formations between a primary amine group in an antibody and the NHS ester at room temperature (Figure 1C). In the last step of the SERS-sensor fabrication the remaining active Au/Ag surfaces was blocked by bovine serum albumin (Figure 1D). Such an antibody-immobilized SERS substrates can be stored at 4°C. Then L-selectin antigen can be captured directly from the plasma samples (Figure 1E).

The protocol of the antibody immobilization, shown on Figure 1, consists of the following steps:

1. *Ozone cleaning*–In corona treater a length of the spark was set to its maximal value, thus the voltage between the high voltage (HV) electrode and ground was set to 45 kV (25 mm spark represents peak voltages of approximately 45 kV, and a 13 mm spark represents a proportional 25 kV). The distance between the sample and HV electrode was 11 mm and the time of modification was 30 seconds. These parameters were used for preparation of all SERS platforms.
2. *Immobilization*–SERS substrates were placed in 0.1 mM of PEG-NHS in PBS buffer solution (1 mL for one substrate) and left in the fridge overnight to spontaneously form bonds with gold substrate in one end and the NHS-ester linkage monolayer in the second end.
3. *Functionalization*–The L-selectin solution containing antibody (20 μg mL^{-1} of L-selectin antibody) was prepared. L-selectin antibody was functionalized onto the prepared substrates (5 μL of L-selectin antibody dropped on the SERS substrate and left for 1 hour). The substrates were rinsed twice with 5 mL of PBS buffer solution.
4. *Surface blocking*–To complete the applied procedure, two additional steps were performed: (a) surface cleaning with 1 M of ethanolamine for few minutes to cap residual NHS ester and (b) the remaining active Au/Ag surfaces was blocked by 5 mL of 2% bovine serum albumin in PBS buffer solution (pH = 7.2) for 30 minutes, and again were rinsed with PBS.

2.4 | SERS and chemometric analysis

The measurements were performed using Bruker's BRAVO Raman spectrometer equipped with SSE (Sequentially Shifted Excitation) to fluorescence quenching, Duo LASER (700–1100 nm) and CCD camera. The power of the excitation light was less than 100 mW for both LASERs and the spectral resolution was 2 to 4 cm^{-1}. The SERS measurements were recorded repeatedly to obtain 10 single measurements for each sample. Using a built-in OPUS software package (Bruker Optic GmbH 2012 version) the recorded Raman spectra were sequentially smoothed with Savitsky-Golay filter, the background was removed using baseline correction (concave rubberband correction; 10 itenary and 64 points), and then the spectra were normalized using a so-called "Min-Max normalization." Afterward, the data were transferred to the Unscrambler software (CAMO software AS, version 10.3, Norway), where the principal component analysis (PCA) was performed. Data were cross validated with applying the uncertainty test (with optimal number of principal components).

3 | RESULTS AND DISCUSSION

3.1 | Characterization of the Au/Ag surfaces: Morphology, enhancement factor and reproducibility

To establish the best condition for SERS substrate preparation, freshly fabricated platforms were characterized using SEM images. The obtained nanostructures of Au/Ag nanocrystals are uniformly covering the whole area of SERS platforms (Figure 2). Diameter of the obtained nanocrystals were estimated based on the ImageJ software in the range of 185 nm ± 65 nm.

The maximal enhancing properties of fabricated SERS platforms were optimized by applying different thicknesses of the sputtered Au/Ag layer, that is, 10, 40, 70 and 100 nm. Freshly prepared platforms with four different thickness of sputtered layer were left for 24 hour in 2 mL of the *para*-mercaptobenzoic acid chosen as standard (*p*-MBA; 10^{-6} M) and afterward the SERS experiments were performed (Figure 1S, Supporting Information). Obtained SERS spectra are dominated by the 1073 cm^{-1} band, which was selected to find the optimal thickness of the sputtered Au/Ag layer. Intensity of this band shows largest gain, that occurs for a thickness of the Au/Ag layer of 100 nm (78 360 counts; cps). However, the Au/Ag platform sputtered with 70 nm layer gave good enough gain (51 760 counts for 1073 cm^{-1} band), in the same order of magnitude. The EF was calculated based on the SERS (*p*-MBA; 10^{-6} M standard solution) and normal Raman spectrum gathered for standard solution and crystals of *p*-MBA (density of 1.19 g/cm^3), respectively. Raman intensity of the corresponding band, observed at 1086 cm^{-1}, was 1131 cps (Figure 1S; Supporting Information). The detailed discussion of the calculation method is presented in the

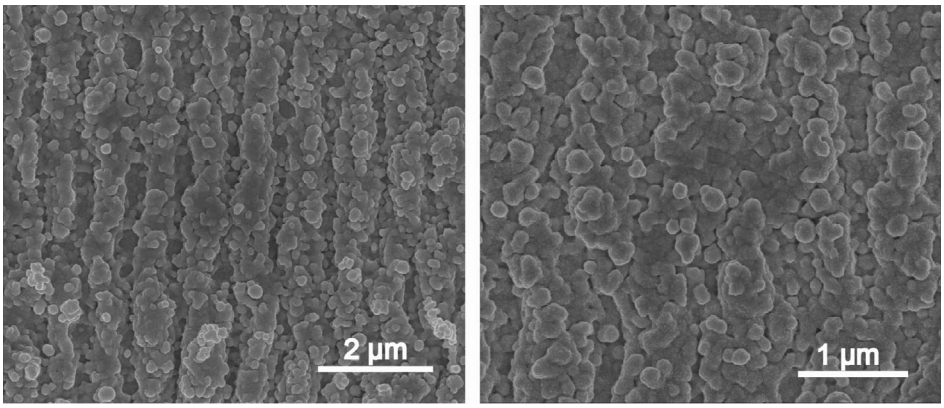

FIGURE 2 SEM images of SERS surface covered with 70 nm of Au/Ag alloy in two different magnifications. SERS, surface enhanced Raman spectroscopy

Supporting Information. For SERS platform covered with 70 nm layer of Au/Ag alloy, and taking into account the representative and intensive band at 1073 cm^{-1} observed in the spectrum (I_{SERS} = 51 760 cps), selected for *EF* calculation, and its band at 1086 cm^{-1} observed in the normal Raman spectrum (I_{Raman} = 1130 cps) calculated $EF = 1.8 \times 10^5$. For SERS platform with 100 nm thicknesses of the sputtered Ag/Au alloy the calculated $EF = 2.7 \times 10^5$. Those *EF* are in the same order of magnitude. To conclude, SERS platforms covered with Au/Ag of 70 and 100 nm layer, revealed comparable and good spectroscopic properties like sensitivity and reproducibility of the SERS signal across the single platform. Therefore, to decrease time of preparation and the cost of whole procedure of the SERS platform fabrication the 70 nm of Au/Ag layer was chosen and used throughout presented experiments.

Moreover, the reproducibility of SERS spectra signal across a single platform was calculated based onto the SD method. Data gathered for the SERS platform with 70 nm of Au/Ag covered with *p*-MBA 10^{-6} M are presented along with the reproducibility of the signal gathered for the immobilized platform covered with L-selectin 100 ng mL^{-1} (Figure 2S, Supporting Information). Calculated SD for *p*-MBA 10^{-6} M based on the intensity of the band at 1073 cm^{-1} is 1.6% in relation to the intensity at the same Raman shift of the average plot. While, for 100 ng mL^{-1} L-selectin, calculation based on the band at 1468 cm^{-1}, gives 0.6% SD in relation to the intensity at the same Raman shift of the average plot. The repeatability of the separated procedures is 7.5 ± 2.5% SD.

3.2 | SERS-based sensor for the L-selectin: Detection limit, specificity and selectivity

The correctness of the applied protocol were tested by comparison the obtained SERS data for the substrate covered with PEG-NHS (immobilization step) and after applying the L-selectin antibody (functionalization step) with the L-selectin antigen captured from two arbitrary selected L-selectin solutions 80 and 1000 ng mL^{-1} (Figure 3SA; Supporting Information). In the low frequency range (below 1200 cm^{-1}) there is no obvious changes in the bands intensity and/or position. The main and the most intensive bands show relation in accordance with studied samples. Accordingly, bands show intensity changing, for example, decreasing (1354, 1644 cm^{-1}) or increasing (1896, 2046 cm^{-1}) due to the functionalization of the SERS platform. Observed changes proved that after the immobilization and the functionalization steps the prepared SERS-sensor captured the L-selectin antigen from studied samples. Moreover, bands at 1600 and 1644 cm^{-1} show intensity changes, in agreement with the level variation of the L-selectin antigen captured by sensor from two 80 and 1000 ng mL^{-1} L-selectin solutions.

Further, a dilution of series of the L-selectin in PBS buffer in the range between 5 and 2000 ng mL^{-1} were prepared in PBS buffer. Each dilution were placed onto active-SERS substrates and left for 30 minute at room temperature. Figure 3A presents the obtained SERS data for increasing concentration of L-selectin in PBS buffer along with SERS data recorded for the plasma of the patient with lung adenocarcinoma. Most intensive bands are due to vibration of lipids (724, 1468 cm^{-1}), tyrosine (644, 858 cm^{-1}) but also some other modes vibration of amide III (1236, 1286 cm^{-1}) and L-tryptophan (724, 1286, 1450, 1580 cm^{-1}). There are no specific or obvious changes of the band intensities due to detected L-selectin level variation. However, in the area of broader band observed at 1468 cm^{-1} with increasing the L-selectin level a small red shifting is observed. For highest studied L-selectin level solution, that is, 2000 ng mL^{-1} an additional small band is revealed; marked as 1450s (L-Tryptophan) in Figure 3A. The Raman bands assignments are presented in Table 1. Due to the fact that, the obtained

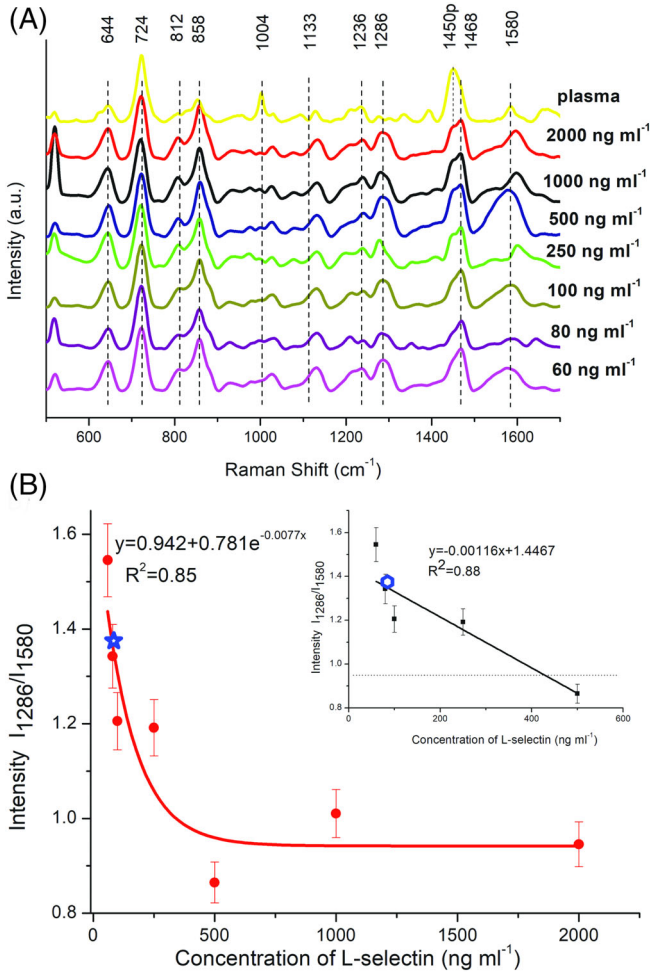

FIGURE 3 A, SERS spectra obtained during detection of L-selectin using SERS-active antibody against that selectin for increasing concentration of L-selectin: 60, 80, 100, 250, 500, 1000, 2000 ng mL^{-1} in PBS buffer along with spectra of the sample collected from patient with adenocarcinoma (plasma). Each spectra were taken after the 30 minutes incubation at room temperature and washing step using the PBS buffer solution. Presented spectra of each L-selectin concentration was averages from 20 measurements in different places across the samples, taken in the mapping mode. B, The calibration curve presents the relationship between the bands intensity (I_{1286}/I_{1580}) versus the L-selectin concentration. The error bars indicate SD of three independent experiments. The star-like mark is inserted from the data obtained for plasma of the patient with lung adenocarcinoma. PBS, phosphate-buffered saline; SERS, surface enhanced Raman spectroscopy

data show only slight spectral differences, therefore to strength spectral analysis and to find sufficient correlation between the L-selectin level and the observed spectral changes of recorded spectra, the ratio of two bands intensities (I_{1286}/I_{1580}) were calculated. The exponential decay calibration curve between the I_{1286}/I_{1580} bands intensities and the L-selectin concentration was fitted

TABLE 1 The Raman bands assignments observed in the SERS spectra of studied samples[33, 36–40]

SERS bands	Compound/assignments
644	Tyrosine
724	Lipids, tryptophan
812, 858	Tyrosine (Fermi resonance ring breathing/ overtone ν_{16})
932, 976	Amide skeleton N—C_α—C stretch (α-helis)
1002, 1008	Phenylalanine (ring breathing mode), tyrosine
1078	Glycogen (C—C)
1130	C—C skeletal stretch trans-conformation
1208	ν(C—CH), Tryptophan, phenylalanine
1236,	Amide III
1286	L-Tryptophan, amide III (α-helis)
1410	$\nu(C{=}O)O^-$ (amino acids aspartic & glutamicacid)
1450	L-Tryptophan, lipids, proteins, δCH_2, δCH_3
1468	Lipids
1552	L-Tryptophan or amide II or protein indole ring
1580	Tryptophan, νC—C in phenylalanine, adenine and guanine (nucleic acid)

Abbreviation: SERS, surface enhanced Raman spectroscopy.

(Figure 3B) and the coefficient of determination (R^2) was calculated as 0.85. This kind of curve fit to the experimental points (calibration curve of exponential decay) is probably due to the SERS-sensor saturating; the amount of the antigen that can be captured is strongly determined by the sensor topography. In other words, the correct operation of the presented SERS-sensor depends on the amount of particles covering it. The detection and the signal is holdup, when to high amount of L-selectin molecules is applied to the sensor. Therefore, a new correlation curve was constructed between the observed signal intensity ratio of the bands at 1286 and 1580 cm^{-1} (shown as insert in Figure 3B). According to presented data the sensor sensitivity is in the range of 60 to 500 ng mL^{-1} L-selectin level (based on the given equation, the higher possible level for $y_0 = 0.96$ is calculated to be 450 ng mL^{-1}). On the other hand, taking into account the presented calibration curves (Figure 3B), 60 ng mL^{-1} L-selectin is on the edge of the detection limit of the presented technology. Thus, the quantitative analysis of plasma with a low concentration of L-selectin (approximately 60 ng mL^{-1}) carries the greatest error. Taking this into account, the range of concentrations is narrowed to 80 ng mL^{-1}. To conclude, the fabricated SERS-sensor is very sensitive for low L-selectin level in

the plasma sample with L-selectin level (80–450 ng mL^{-1}) strongly correlated with existing tumors.

It is already known that the soluble form of L-selectin can be easily measured qualitatively in the plasma, thus in order to verify effectivity of the constructed calibration curve two biological plasma samples were studied (from healthy and from patient with adenocarcinoma of the lung). Based on the recorded SERS spectra, the I_{1286}/I_{1580} bands intensities ratio calculated for healthy sample is 0.58, which is below the cutoff line of the constructed curve. Such L-selectin level is quite high, as already observed in the plasma of healthy individuals, where mean level of L-selectin is 1.6 ± 0.8 mg mL^{-1}.[35] On the other hand, those bands intensities ratio calculated for SERS plasma sample with adenocarcinoma is 1.35 (points marked as star-shape in Figure 3B). Thus, based on the obtained equation of the calibration curve, the designated level of captured L-selectin in the serum sample is 85 ng mL^{-1}. SERS data gathered for the second adenocarcinoma sample, indicate that plasma L-selectin level is below 60 ng mL^{-1}. Therefore, this sample is not marked in the presented plots on Figure 3B.

Two of those biological samples (plasma of a healthy patient and a patient with lung adenocarcinoma) were additionally verified using human L-selectin enzyme-linked immunosorbent assay (ELISA, Sigma–Aldrich). However, the ELISAs can be used only for research not for diagnostic procedures and in addition, commercially available ELISAs are sensitive only in the low concentration region below 58 ng mL^{-1}. Since serum or plasma samples must be diluted, it is not possible to accurately calculate the L-selectin level on the basis of the determined curve (determined curves are differ at low and high concentrations). In this sense, the obtained results only indicate a tendency, for example, which sample has a lower or higher of L-selectin level–enable only qualitative, not quantitative analysis. Herein, for the ELISA L-selectin analysis the plasma samples (from healthy and lung adenocarcinoma patients) were diluted as 1:100. Then, the absorbance of all prepared samples (standards and biological samples) was measured at 450 nm. Based on the gathered data, the ELISA calibration curve was constructed (Figure 4S; Supporting Information). The absorbance level recorded for biological samples are marked as stars. The absorbance of plasma from healthy patient is higher, then the absorbance of plasma with adenocarcinoma. To summarize, the curve obtained from the ELISA are in agreement to the data calculated using SERS-based method in the sense of tendency.

The specificity and the selectivity of the fabricated L-selectin SERS-sensor was tested by immersing freshly prepared three SERS-sensors in 5 mL of 250 ng mL^{-1} of P-, E- and L-selectins solutions for 30 minutes (separate sensor for each solution). The obtained SERS data were compared with spectra of 250 ng mL^{-1} of L-selectin (Figure 5SA; Supporting Information). There are some differences between the SERS spectra observed especially in the position of bands at 1208 cm^{-1}, but mostly those small differences are due to bands intensities at 976, 1078, 1208 and 1236 cm^{-1}. Such a result indicate good selectivity of fabricated L-selectin SERS-sensor. According to chemical supplied source (Tocris Bioscience, Bristol, UK), used L-selectin antibody may attach other L-selectin human proteins including P- and E-selectins; however, as it is observed in SERS data, some differences among their spectra exist. Moreover those spectral differences in the SERS data were tested using principal component analysis (Figure 5SB; Supporting Information). Calculated scores in the PC1 vs PC2 plots are revealed in separated, different areas, indicating differences in the attachment of each P, E and L-selectins to the fabricated SERS-sensor. Thus, despite the coexistence of P- and E-selectins in the clinical samples the high sensitivity is obtained for the presented L-selectin SERS-sensor.

3.3 | PCA analysis of SERS data

In the next step, to strength the elaborated method of L-selectin determination, SERS data were analyzed using multivariate analysis based on PCA. PCA analysis transforms a large number of original Raman data (correlated variables) into a smaller number of uncorrelated variables called principal components (PCs). Calculated scores show how the studied data are related to each other, while the loadings reveal the importance of the original variables for the patterns seen in the scores. In other words, any important changes, differences or similarities found in the SERS data set, that influences computed differentiation between analyzed spectra, are shown as the most weighted variables in the loadings. Similarly, as the SERS data analyzed above, in order to prove that the prepared SERS-sensor captured the L-selectin antigen from the studied sample PCA analysis was done over the SERS data of sensors after immobilization and functionalization steps along with the SERS data of plasma collected from patient with lung adenocarcinoma (Figure 3SB, Supporting Information). Resultant scores are divided by PC1-1 and PC-2 axes. Scores obtained SERS-sensors after immobilization and functionalization are on the same, negative side of PC-2 axis, while scores with already captured L-selectin antigens, from studied the adenocarcinoma sample and 500 ng mL^{-1} L-selectin solution, are on the positive side of PC-2 axis. Moreover, scores gathered for the sample

without captured antigen are very close to each other, whereas some distance is observed among the scores calculated for samples with captured L-selectin antigen. Between those two samples some obvious differences exist first and the most important is that one is the biological plasma and the second is solution with artificially added L-selectin in given amount. Therefore, their calculated scores are in distance, divided by PC-1 axis.

Plots of PC-1 and PC-2 scores calculated for all studied L-selectin concentration (from 60 to 2000 ng mL^{-1}) presented on Figure 6S (Supporting Information) indicate, that the first and the second principal components (PC1 + PC2) carries 77% of variance among studied samples. Calculated scores of high L-selectin concentrations (500 and 1000 ng mL^{-1}) are separated from the scores of smaller L-selectin concentration (60, 80, 100 and 250 ng mL^{-1}) by the PC-1 axis. However, the scores of 2000 ng mL^{-1}, are in the centre of both scales and prove difficultness in proper differentiation and discrimination. What indicate correctness in calibration curve analysis and usages limit of the fabricated SERS-sensor to 80–450 ng mL^{-1} L-selectin level (Figure 3B). Therefore, further PCA analysis was reduced to the 60 to 500 ng mL^{-1} level of L-selectin concentration in the captured solutions (Figure 4). For that region, the calculated scores prove, that the first and the second principal components (PC1, PC2) are the most significant and explain 80%, of the variance in the data. As can be seen, obtained scores are gathered in the separated groups. Scores calculated for 60 ng mL^{-1} L-selectin solution are close to the PC-1 and PC-2 axes centre, what can be caused by not sufficient differences detected in their spectral features in comparison to the spectra of other studied samples. That is also in agreement with constructed linear calibration curve (the points related to I_{1286}/I_{1580} ratio for SERS spectra of the 60 ng mL^{-1} sample are above the calibration curve; Figure 3B, insert).

Based on the PC-1 loadings, PCA technique allows to find the most prominent bands, that strongly influenced obtained differentiation, that is, 1520, 1450, 1404, 1288, 1238 and 864 cm^{-1}(Figure 6S; Supporting Information and Figure 4, respectively). The most weighted variables, assigned and presented along with theirs weightings, are nicely correlated with SERS spectra (Figure 2A), as for example broad band at 1580 cm^{-1} or at 1468, 1286 cm^{-1} show intensity and shifting changes with L-selectin level variation.

Interestingly, intensities of the bands at 1286 and 1580 cm^{-1} (Figure 3A), observed in the SERS data and used to determine the calibration line, and accordingly to PCA calculation the corresponding variables at 1580 and 1286 cm^{-1} (Figure 4B) are largely influence the calculated discrimination. Those variables are strongly related

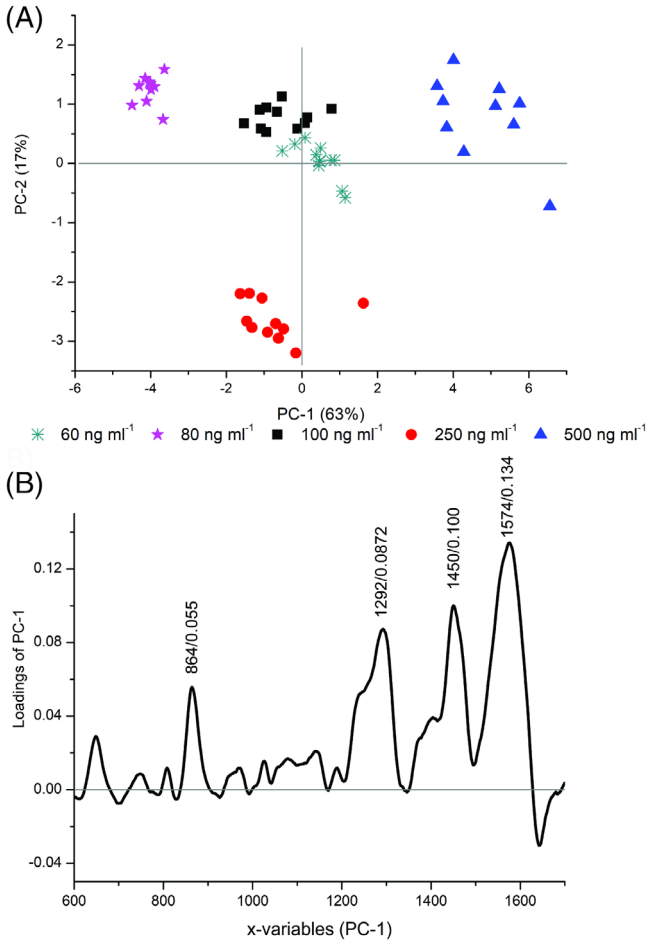

FIGURE 4 PC-1 vs PC-2 scores of L-selectin various concentration solution in the 60 to 500 ng mL^{-1} region, A; together with the corresponding PC-1 loadings, **B**. The most weighted variables are presented together with their weighting. PC, principle components

to L-tryptophan/tryptophan vibrations which is one of the essential amino acid for humans and are directly connected to L-selectin level in the studied samples (healthy or tumor). Till now the lower degradation of tryptophan caused by the enzyme indoleamin (2,3)-dioxygenase stimulated by Th1 immune response (IDO) was observed in colorectal,[41] colon[42] and breast cancer[43] and was linked to cancer development and progression.[41]

To conclude, to use L-selectin level in the blood and lymph for early- stage tumor diagnosis, it is important to develop sensing systems to detect L-selectin at low (below 700 ng mL^{-1}) level. Such range is highly desired cause the commercially available L-selectin sensors allow to detect L-selectin in the lower region of the possible scale (e.g. used ELISA are sensitive to around 20 ng mL^{-1}) and it cannot sense the beginning of the changes of the L-selectin level in the body (in healthy individuals L-selectin level ranges 700 to 1500 ng mL^{-1}). Fabricated SERS-based sensor can be used directly to record the

SERS data, and based on the equation of the determined calibration curve it is possible to calculate the amount of L-selectin in the plasma sample.

4 | CONCLUSIONS

The presented SERS-based sensor for detecting L-selectin levels from plasma samples allows to observe changes in the reduced level of L-selectin (80–450 ng mL^{-1}) related to the development of benign and malignant neoplastic diseases. To determine the calibration curve the intensity ratio of the two bands (I_{1286}/I_{1580}), observed in SERS spectra, which accordingly to PCA calculation have a large impact on the calculated data, was selected. Serum and plasma samples do not require any pretreatment for analysis (no dilution compared to commercially available ELISAs). Therefore, the results (L-selectin level in plasma samples) can be read directly from the constructed curve, which indicates the possibility to use elaborated method in medical diagnostics.

ACKNOWLEDGMENTS

Authors would like to thanks dr Izabela Chmielewska for providing the biological samples and the National Science Centre, OPUS XIII 2017/25/B/ST4/01109.

DATA AVAILABILITY STATEMENT

Data available in article supplementary material.

ORCID

Aneta Aniela Kowalska https://orcid.org/0000-0002-1904-9459

REFERENCES

[1] O. Sobolev, P. Stern, A. Lacy-Hulbert, R. O. Hynes, *Cancer Res.* **2009**, *69*, 2531.
[2] K. Ley, G. S. Kansas, *Nat. Rev. Immunol.* **2004**, *4*, 325.
[3] C. Grégoire, L. Chasson, C. Luci, E. Tomasello, F. Geissmann, E. Vivier, T. Walzer, *Immunol. Rev.* **2007**, *220*, 169.
[4] M. A. Morris, K. Ley, *Curr. Mol. Med.* **2004**, *4*, 431.
[5] T. N. Mayadas, R. C. Johnson, H. Rayburn, R. O. Hynes, D. D. Wagner, *Cell* **1993**, *74*, 541.
[6] M. L. Arbones, D. C. Ord, K. Ley, H. Ratech, C. Maynard-curry, G. Otten, D. J. Capon, T. F. Teddert, *Immunity* **1994**, *1*, 247.
[7] S. D. Robinson, P. S. Frenette, H. Rayburn, M. Cummiskey, M. Ullman-Culleré, D. D. Wagner, R. O. Hynes, *Proc. Natl. Acad. Sci. U. S. A.* **1999**, *96*, 11452.
[8] K. Ley, *Trends Mol. Med.* **2003**, *9*, 263.
[9] N. A. Raffler, J. Rivera-Nieves, K. Ley, *Drug Discovery Today: Ther. Strategies* **2005**, *2*, 213.
[10] Q. Wang, X. N. Tang, M. A. Yenari, *J. Neuroimmunol.* **2007**, *184*, 53.
[11] H. Läubli, J. L. Stevenson, A. Varki, N. M. Varki, L. Borsig, *Cancer Res.* **2006**, *66*, 1536.
[12] K. F. Boligan, C. Mesa, L. E. Fernandez, S. Von Gunten, *Cell. Mol. Life Sci.* **2015**, *72*, 1231.
[13] S. S. Pinho, C. A. Reis, *Nat. Rev. Cancer* **2015**, *15*, 540.
[14] L. Borsig, *Glycobiology* **2019**, *28*, 648.
[15] S. D. Rosen, *Annu. Rev. Immunol.* **2004**, *22*, 129.
[16] M. Sperandio, M. L. Smith, S. B. Forlow, T. S. Olson, L. Xia, R. P. McEver, K. Ley, *J. Exp. Med.* **2003**, *197*, 1355.
[17] S. R. Barthel, J. D. Gavino, L. Descheny, C. J. Dimitroff, *Expert Opin. Ther. Targets* **2008**, *11*, 1473.
[18] C. Granert, J. Raud, X. Xie, L. Lindquist, L. Lindbom, *J. Clin. Invest.* **1994**, *93*, 929.
[19] C. E. Wilcox, A. M. V. Ward, A. Evans, D. Baker, R. Rothlein, J. L. Turk, *J. Neuroimmunol.* **1990**, *30*, 43.
[20] W. M. Clark, J. D. Lauten, N. Lessov, W. Woodward, B. M. Coull, *Mol. Chem. Neuropathol.* **1995**, *26*, 213.
[21] D. B. Majchrzak-Baczmańska, E. Głowacka, M. Wilczyński, A. Malinowski, *Prz. Menopauzalny* **2018**, *17*, 11.
[22] D. Choudhary, P. Hegde, O. Voznesensky, S. Choudhary, S. Kopsiaftis, K. P. Claffey, C. C. Pilbeam, J. A. Taylor III., *Physiol. Behav.* **2016**, *176*, 139.
[23] A. Ivetic, H. L. H. Green, S. J. Hart, *Front. Immunol.* **2019**, *10*, 1.
[24] P. J. Cywiński, L. Olejko, H. G. Löhmannsröben, *Anal. Chim. Acta* **2015**, *887*, 209.
[25] K. I. Nishijima, M. Ando, S. Sano, A. Hayashi-Ozawa, Y. Kinoshita, S. Iijima, *Immunology* **2005**, *116*, 347.
[26] E. C. Le Ru, P. G. Etchegoin, *MRS Bull.* **2013**, *38*, 631.
[27] L. M. Almehmadi, S. M. Curley, N. A. Tokranova, S. A. Tenenbaum, I. K. Lednev, *Sci. Rep.* **2019**, *9*, 1.
[28] D. Cialla, S. Pollok, C. Steinbrücker, K. Weber, J. Popp, *Nanophotonics* **2014**, *3*, 383.
[29] C. Chen, W. Liu, S. Tian, T. Hong, *Sensors* **2019**, *19*, 19.
[30] E. Witkowska, K. Niciński, D. Korsak, B. Dominiak, J. Waluk, A. Kamińska, *J. Biophotonics* **2020**, *13*, 1.
[31] A. Kamińska, E. Witkowska, K. Winkler, I. Dziecielewski, J. L. Weyher, J. Waluk, *Biosens. Bioelectron.* **2015**, *66*, 461.
[32] K. Niciński, J. Krajczewski, A. Kudelski, E. Witkowska, J. Trzcińska-Danielewicz, A. Girstun, A. Kamińska, *Sci. Rep.* **2019**, *9*, 1.
[33] A. A. Kowalska, S. Berus, A. Szleszkowski, A. Kamińska, K. Kmiecik, T. J. Ratajczak-Wielgomas, Ł. Zadka, *Spectrochim. Acta, Part A* **2019**, *231*, 117769.
[34] T. Szymborski, Y. Stepanenko, P. Piecyk, K. Niciński, A. Kamińska, Patent Application P.434300 2020.
[35] B. Schleiffenbaum, O. Spertini, T. F. Tedder, *J. Cell Biol.* **1992**, *119*, 229.
[36] J. Dybas, K. M. Marzec, M. Z. Pacia, K. Kochan, K. Czamara, K. Chrabaszcz, E. Staniszewska-Slezak, K. Malek, M. Baranska, A. Kaczor, *Trends Anal. Chem.* **2016**, *85*, 117.
[37] C. G. Atkins, K. Buckley, M. W. Blades, R. F. B. Turner, *Appl. Spectrosc.* **2017**, *71*, 767.
[38] B. Hernández, F. Pflüger, A. Adenier, S. G. Kruglik, M. Ghomi, *J. Phys. Chem. B* **2010**, *114*, 15319.
[39] J. De Gelder, K. De Gussen, P. Vandenabeele, L. Moens, *J. Raman Spectrosc.* **2007**, *38*, 1133.
[40] R. Tuma, *J. Raman Spectrosc.* **2005**, *36*, 307.

[41] A. Huang, D. Fuchs, B. Widner, C. Glover, D. C. Henderson, T. G. Allen-mersh, *Br. J. Cancer* **2002**, *86*, 1691.
[42] X. Li, T. Yang, S. Li, D. Wang, Y. Song, S. Zhang, *Laser Phys.* **2016**, *26*, 035702.
[43] D. E. Lyon, J. M. Walter, A. R. Starkweather, C. M. Schubert, N. L. McCain, *BMC. Res. Notes* **2011**, *4*, 156.

SUPPORTING INFORMATION

Additional supporting information may be found online in the Supporting Information section at the end of this article.

How to cite this article: Kowalska AA, Nowicka AB, Szymborski T, Piecyk P, Kamińska A. SERS-based sensor for direct L-selectin level determination in plasma samples as alternative method of tumor detection. *J. Biophotonics*. 2021; 14:e202000318. https://doi.org/10.1002/jbio.202000318